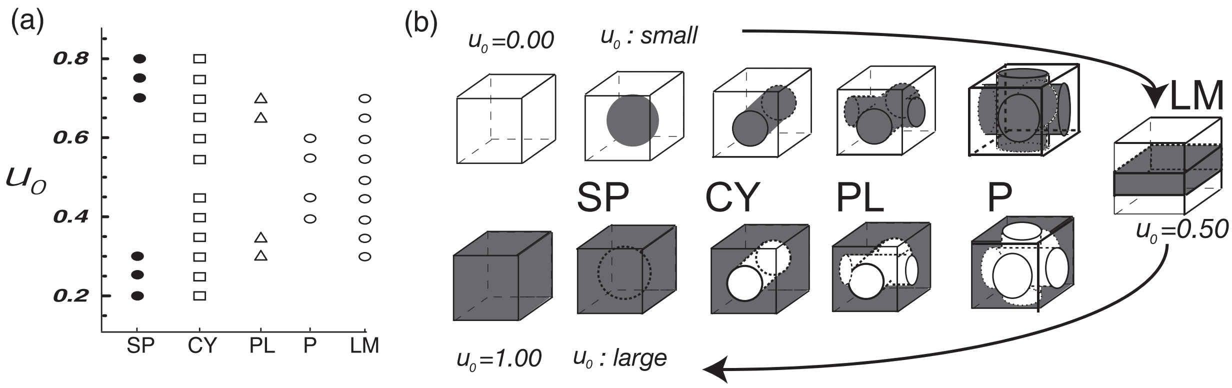

Fig. 1. (a) Five stationary solutions for $D_u = 1.0$, $D_c = 50.0$, $\beta = 10.0$, $k^2 = 50.0$, and $\lambda = 40.0$. The explanations of SP, CY, PL, P and LM are provided in the text. (b) Schematically showing the obtained patterns SP, CY, PL, P and LM.

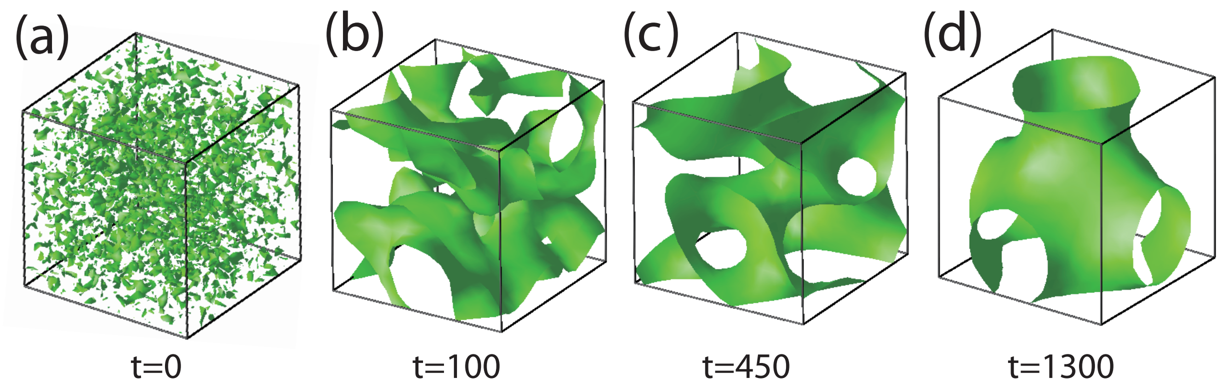

Fig. 2. Time evolution of P-surface for $u_0 = 0.45$ and $L = \delta x N$ with $\delta x = 0.70$ and $N = 32$. The other parameters are same as in Fig. 1. In order to make the initial randomness visible, the domain in (a) represents the isosurface of $u = 0.45060$, whereas those in (b)–(d) represent the isosurfaces of $u = 0.45$.

to discretize the spatial derivatives was also applied.

We start with the uniform solution $(u, c) = (u_0, \lambda u_0/k^2)$ in an unstable condition with a small superimposed random perturbation. As the global existence of solution in Eqs. (1) and (2) was shown analytically (Hillen and Painter, 2001), the distributions continuously evolve without blow up of distributions, leading to the gradual aggregation of cell density of u.

The asymptotic stationary solutions obtained numerically are summarized in Fig. 1, where a lot of random initial conditions and δx were given for a given value of u_0. It should be noted that this set of simulations is very systematic and detailed. For example, we performed simulations for $u_0 = 0.30$ starting from 5 different random initial conditions and for $200 = 5 \times 40$ values of $L = \delta x N$. This implies that there are independent runs for only one value of u_0.

It is found that three or four different patterns are obtained for in Fig. 1(a). The abbreviations LM, CY, and SP mean lamellar, cylinder, and sphere, respectively. The remaining P and PL are explained below.

The formation of P for $u_0 = 0.45$ is displayed in Fig. 2. Figures 3(a) and (b) shows the obtained patterns translated the mass of center of the patter to the center of cubic, and viewed in different two directions. Figure 3(c) shows the stationary profiles of u and c measured along the red arrow shown in Figs. 3(a) and (b). It should be noted that the distributions have sharp interfaces separating between two domains. This pattern is composed of surfaces made of six cylinders as shown in Figs. 2(d) and 3. This pattern is called Schwarz' primitive surface (P-surface), which was first described by Hermann A. Schwarz (1890). The interest in this surface in those days was due to the experimental observation that bi-layers of lipids or surfactants in water solutions form at suitable thermodynamic conditions ordered bi-continuous structures (Luzzati and Spegt, 1867). In the case of $u_0 = 0.55$, the distributions are upside down. The P-surface is known as one of the minimal surfaces with the average curvature equal to zero everywhere. This pattern is a new one found in the full 3D computation in nonequilibrium systems.

The asymptotic pattern PL for $u_0 = 0.35$ is shown in Fig. 4. This pattern is composed of surfaces intersected with four cylinders. When PL connected periodically, the patterns are composed by the lamellar with holes. Therefore, we called PL as perforated lamellae. The inside of perforated lamellae has high density, whereas the remaining space has low density. In the case of $u_0 = 0.65$, the distributions are upside down.

3. Stability Analysis of Obtained Patterns

As mentioned above, some patterns can be obtained for same u_0. One of the basic problems is to determine the most stable structure. However, this is highly nontrivial be-